GSICS-MW Lunar Calibration Working Group Progress Report

Presented by: Hu (Tiger) Yang
UMD/CISESS
huyang@umd.edu

With Contributions from Active Member:

Martin Burgdorf, Hamberg University
Thomas Mueller , Max Planck
Yang Guo   , CMA
Niutao Liu   , Fudan University
Tim Hewison   , EuMetSat
Hao Liu   , NSSC
Hu (Tiger) Yang, UMD
Shengli Wu   , CMA
Juyang Hu   , CMA

03/19, 2025

Working Scope of the Group

- **Microwave lunar RTM model development**

    ✦ Theoretical model development and inter comparison

    ✦ RTM model validation with satellite observations

- **Lunar radiance measurements based on the satellite observations**

    ✦ Lunar satellite observation calibration

    ✦ Sensor related uncertainty in Lunar radiance measurements

- **Lunar observation applications**

    ✦ Antenna beam pointing/Geolocation accuracy evaluation

    ✦ Instrument long-term gain stability evaluation

    ✦ Inter-satellite calibration

Achievements and Progress

Action Items	Person	Status	Comments
Create a sharing space in GitHub for code and document exchange	Tiger Yang	Done	The ATMS Calibrated lunar RTM has been shared to the group through Github
Provide the satellite Moon Tb datasets for the community	Martin/Tiger	Done	Datasets from MHS and ATMS have been shared with the group
Develop a community microwave lunar RTM for current low-resolution sounding instrument calibration	Tiger Yang	Done	A calibrated lunar RTM (CMLRTM) has been developed and shared with the member of lunar calibration group
Develop an open source high-resolution community microwave lunar RTM for current and future microwave sounding instruments	Team efforts	In progress	Reference truth datasets have been collected based on satellite observations. A open-source lunar RTM frame work has been developed for the new model. Working on high-resolution model inputs
Implement the MLRTM in LI correction for satellite on-orbit calibration	Team efforts	In progress	

Highlights of the Research Work in Microwave Lunar Calibration Group

- Microwave Lunar RTM study

- Reference truth from the satellite observations

- Application of microwave lunar model in instrument calibration

- Ground-based microwave lunar cal/val for future instruments

Thermophysical Model (TPM) (Thomas Muller)

- **Model references:**
  - Lagerros (1996, 1997, 1998); Müller & Lagerros (1998, 2002); Müller (2002)
  - Müller, Burgdorf et al. (2021): "The Moon at thermal infrared wavelengths: a benchmark for asteroid thermal models", A&A 650, A38

- **Model aspects:**
  - uses the true illumination and observing geometry (as seen from satellite)
  - considers 1-d heat conduction, shadowing and self-heating
  - Moon is modelled as an oblate spheroid with r_{equ}=1738.1 km and r_{pol}=1736.0 km (r_{equ}/r_{pol} = 1.0012), spin pole at $(\lambda,\beta)_{ecl}$ = (88.43°, 214.45°), P_{syn} = 29.530589 days, with a thermal inertia of 55 tiu (Hayne et al. 2017), and a surface roughness of 32° (Rozitis & Green 2012; Bandfield et al. 2015), absolute magnitude of -0.089 mag (Bowell et al. 1989), and a phase integral of q=0.43 (Muinonen et al. 2010), visual geometric albedo 0.12 (NASA Moon factsheet)
  - Bolometric and spectroscopic (hemispherical) emissivities
  - The "effective MW emissivity" depends on the frequency and phase angle
  - → TPM T_B (at a given frequency) is not a simple function of phase angle (influence of different Sun-Moon distances between 0.98 and 1.02 au)

Temperature [K]

400
350
300
250
200
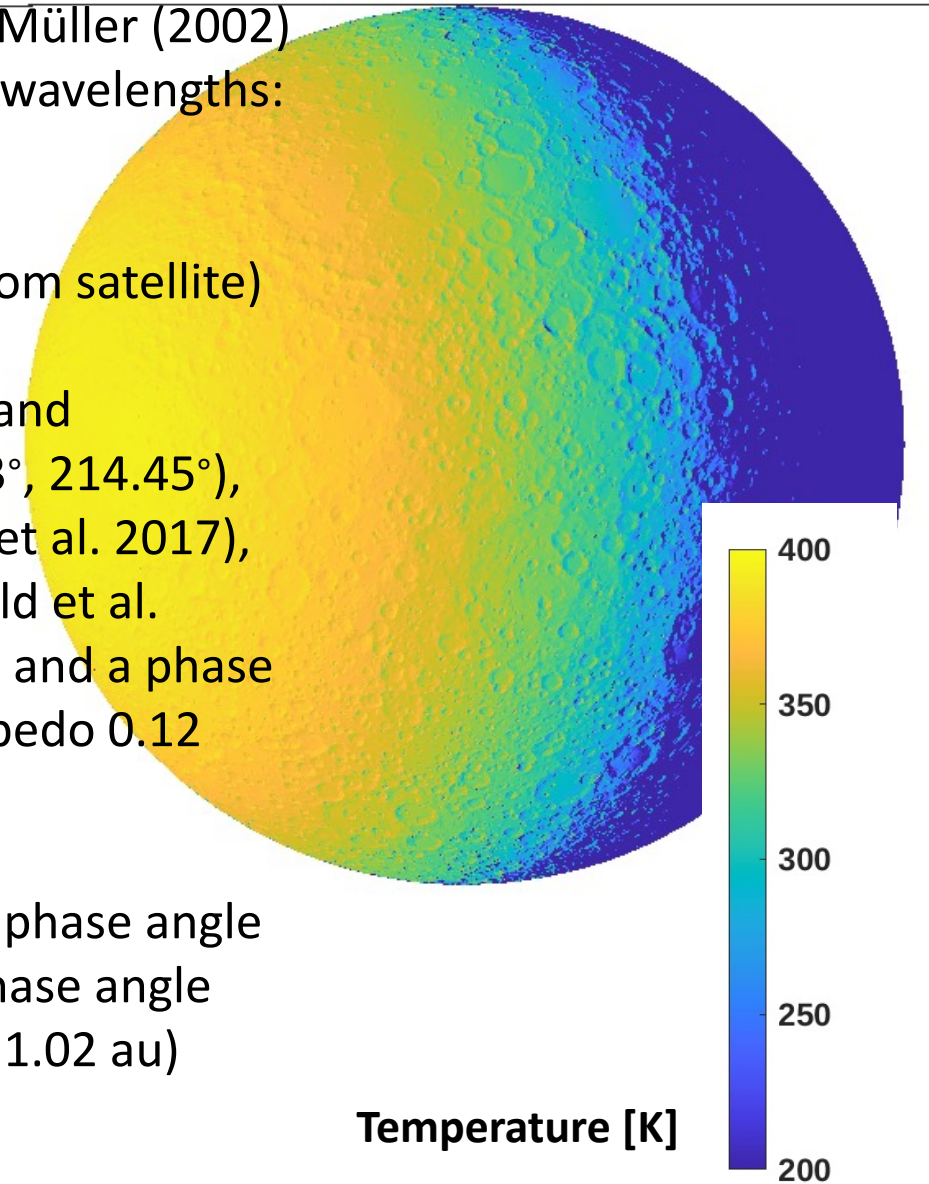
# RTM Model Simulation for Lunar Microwave Emission (Tiger Yang)
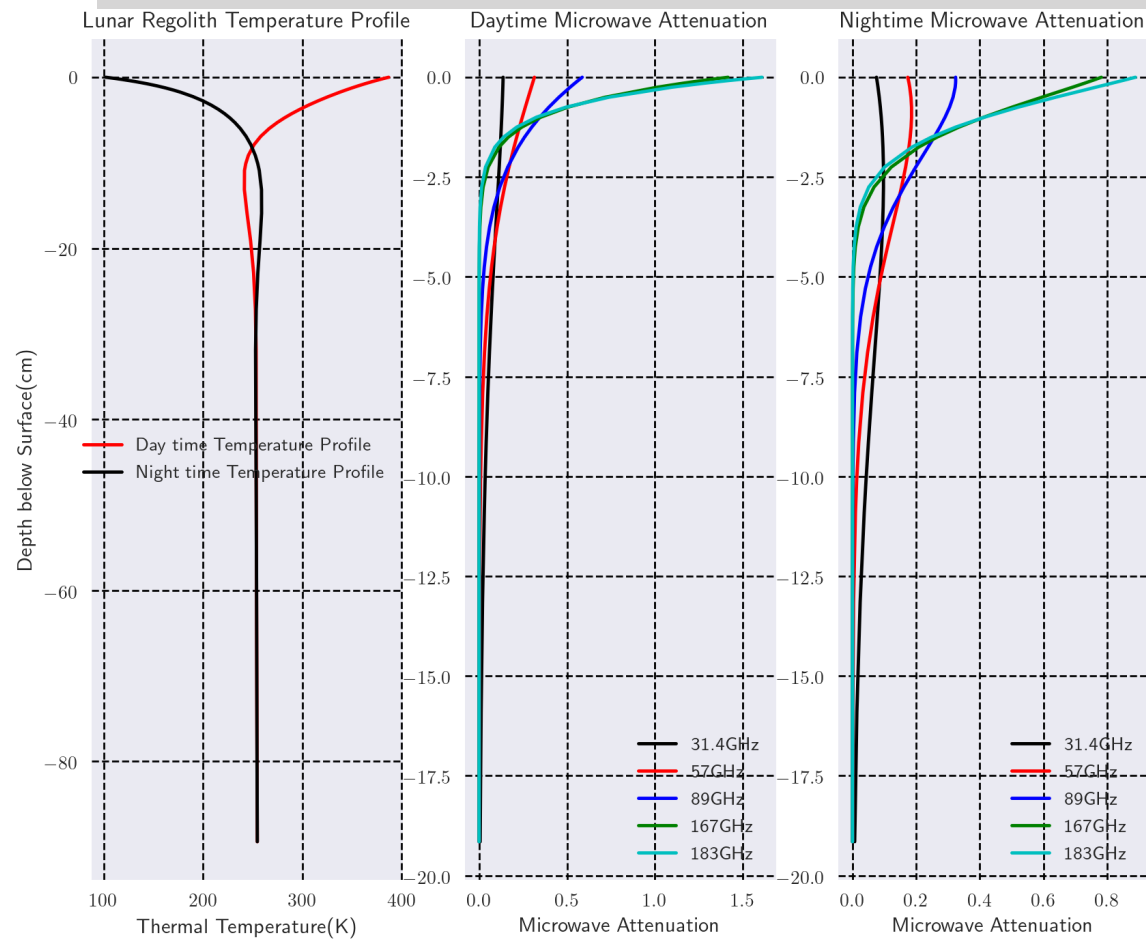
Microwave brightness temperature of lunar emission can be calculated as convolution of microwave electrical loss with lunar regolith temperature profile over different depth(Keihm, 1984)
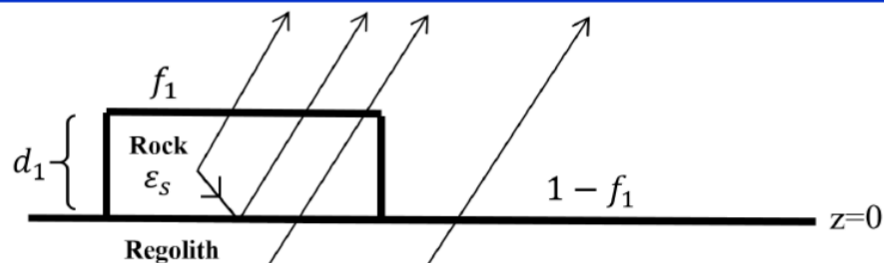
$$TB(\lambda) = E_\lambda \int_0^\infty K_\lambda \sec(\theta_i) \cdot T(z) \cdot e^{- \int_0^z K_\lambda(z') \sec(\theta_i)} dz \tag{1}$$

The discrete form can be written as weighting sum of thermal temperature at each layer:

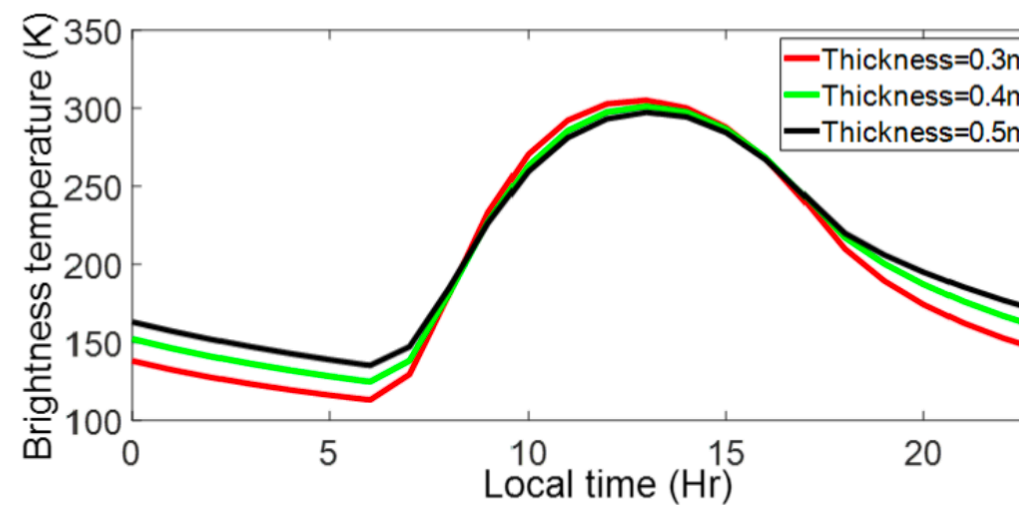$$TB(\lambda) = E_\lambda \sum_{i=1}^{i=n} w_i * T_i \tag{2}$$
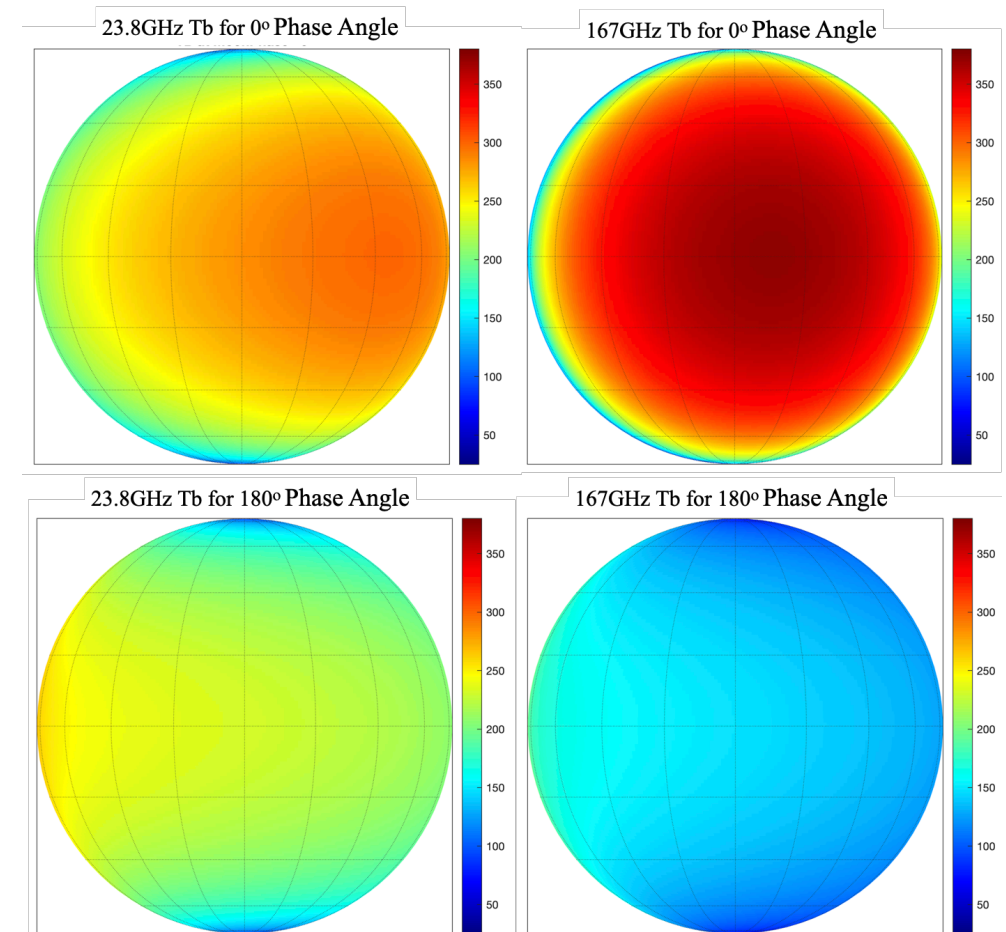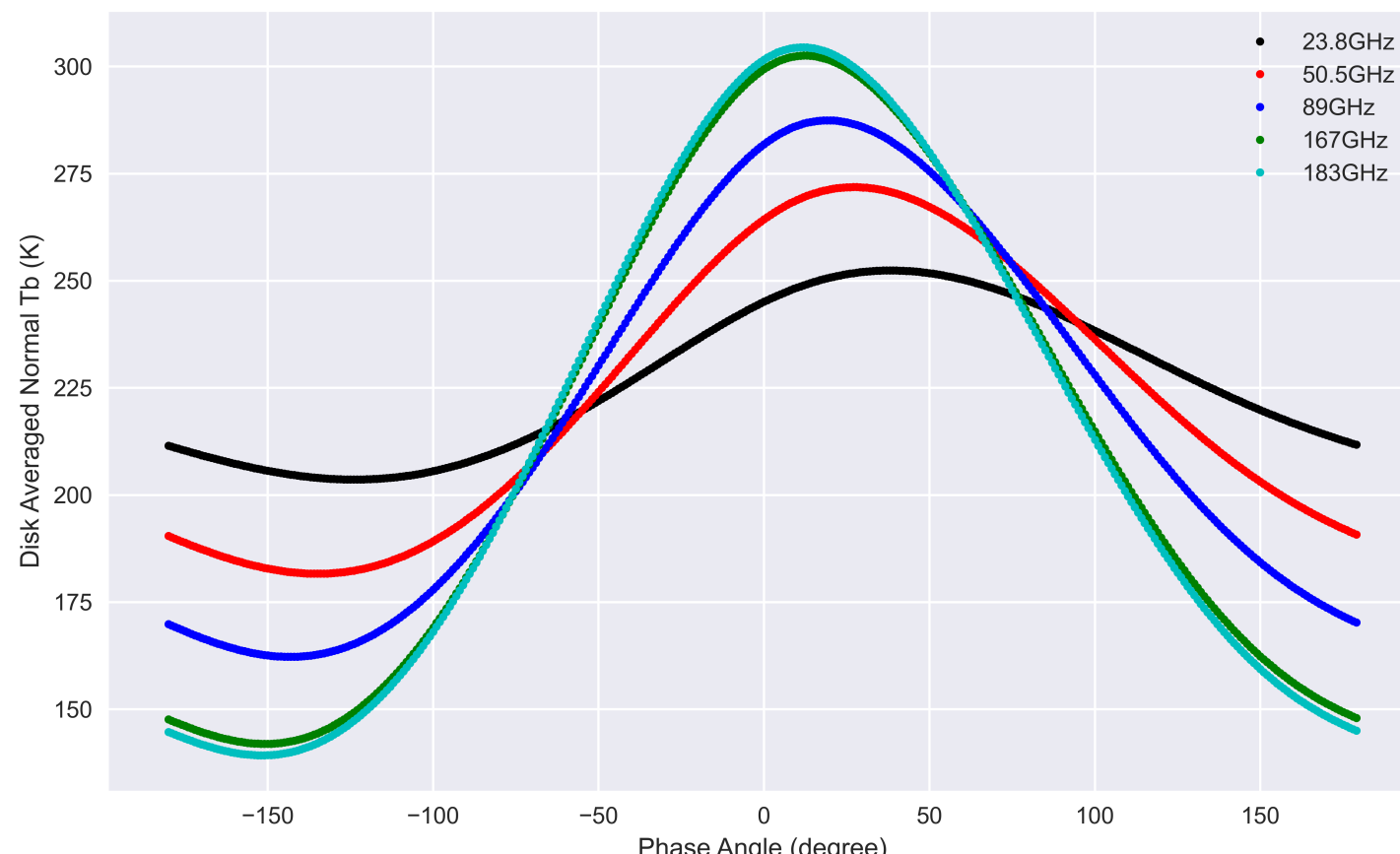
Microwave radiation modeling of rocks (Niutao Liu)

Two-layer model

$$
\begin{aligned}
T_B(0) = & \; f_1 \times [1 - R_0(0)] \cdot \int_0^{d_1} \kappa_a(z) T(z) e^{-\int_z^{d_1} \kappa_a(z')dz'} dz \\
& + f_1 \times [1 - R_0(0)] \cdot R_1(0) \\
& \cdot e^{-\int_0^{d_1} \kappa_a(z')dz'} \cdot \int_0^{d_1} \kappa_a(z) T(z) e^{-\int_0^z \kappa_a(z')dz'} dz \\
& + f_1 \times [1 - R_0(0)][1 - R_1(0)] \\
& \cdot e^{-\int_0^{d_1} \kappa_a(z')dz'} \int_{-\infty}^0 \kappa_a(z) T(z) e^{-\int_z^0 \kappa_a(z')dz'} dz \\
& + (1 - f_1) \times [1 - R_2(0)] \int_{-\infty}^0 \kappa_a(z) T(z) \\
& \cdot e^{-\int_z^0 \kappa_a(z')dz'} dz \quad\quad\quad\quad (10)
\end{aligned}
$$

MW TB of rocks 24° N

The simulated microwave brightness temperature of the rock is related to the thickness, as the thickness affects the physical temperature.

Unlike the half-space lunar soil model, the two layer model contains upgoing radiation from the rock, downgoing radiation and upgoing radiation from the lunar soil.
The four terms in (10), correspondingly, represent the four arrows described in the figure.
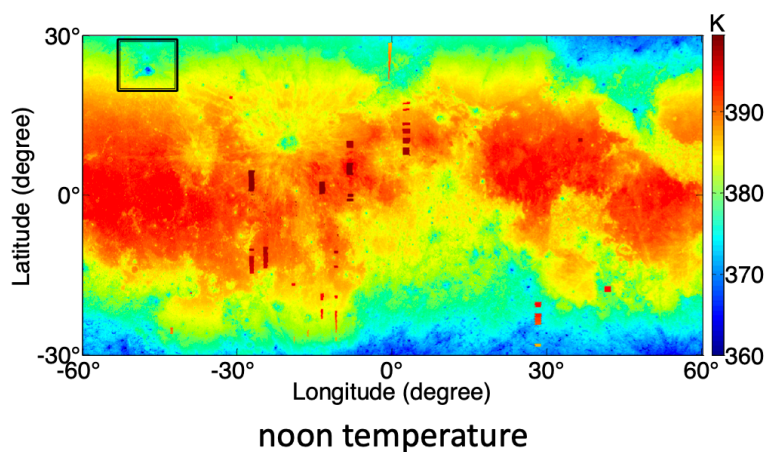
noon temperature
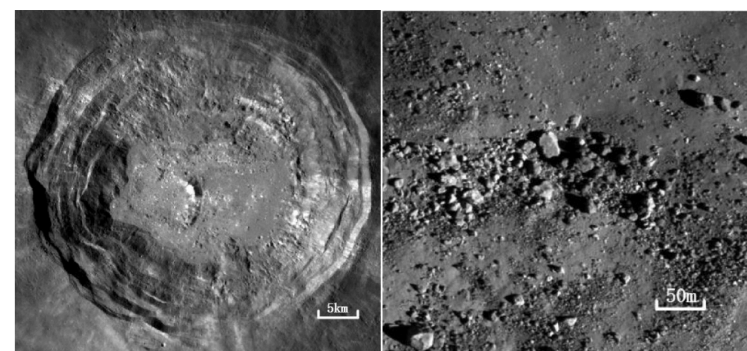
optical image

Aristarchus crater locates at 24°N, 47°W and is about 40km in diameter. The interior of the crater is abundant in rocks.

(Provided by M.Burgdorf)

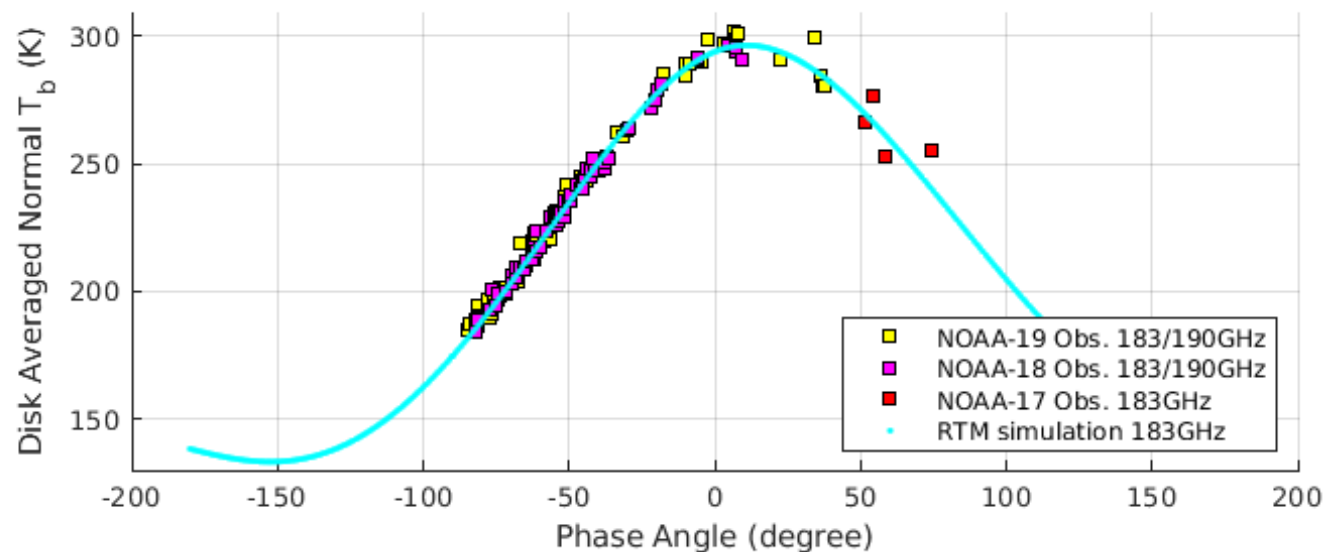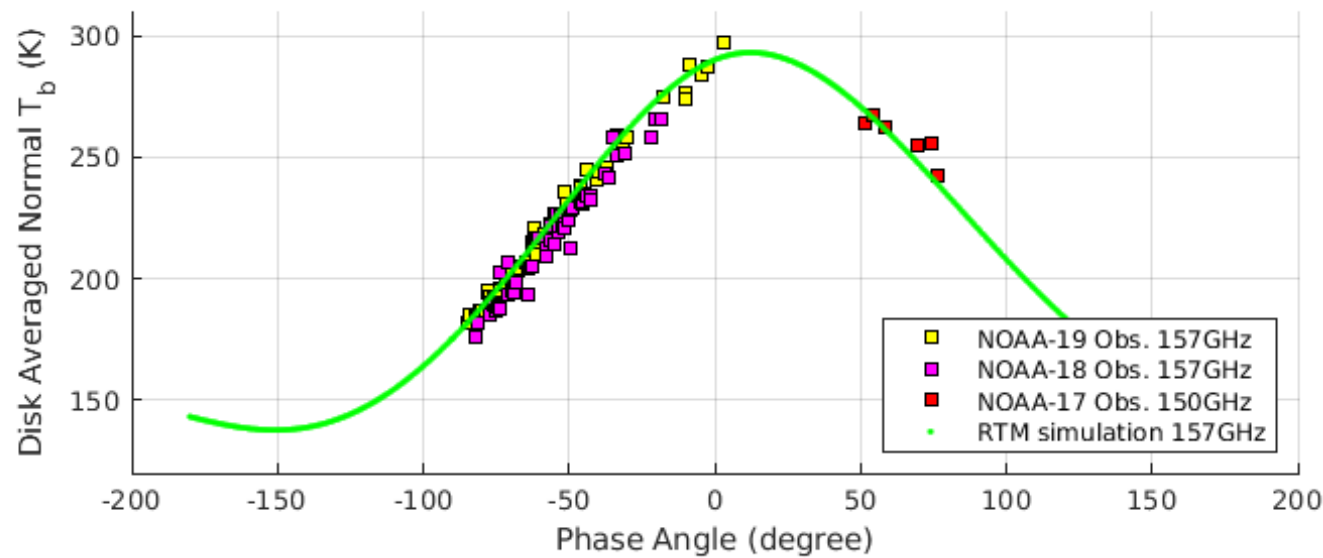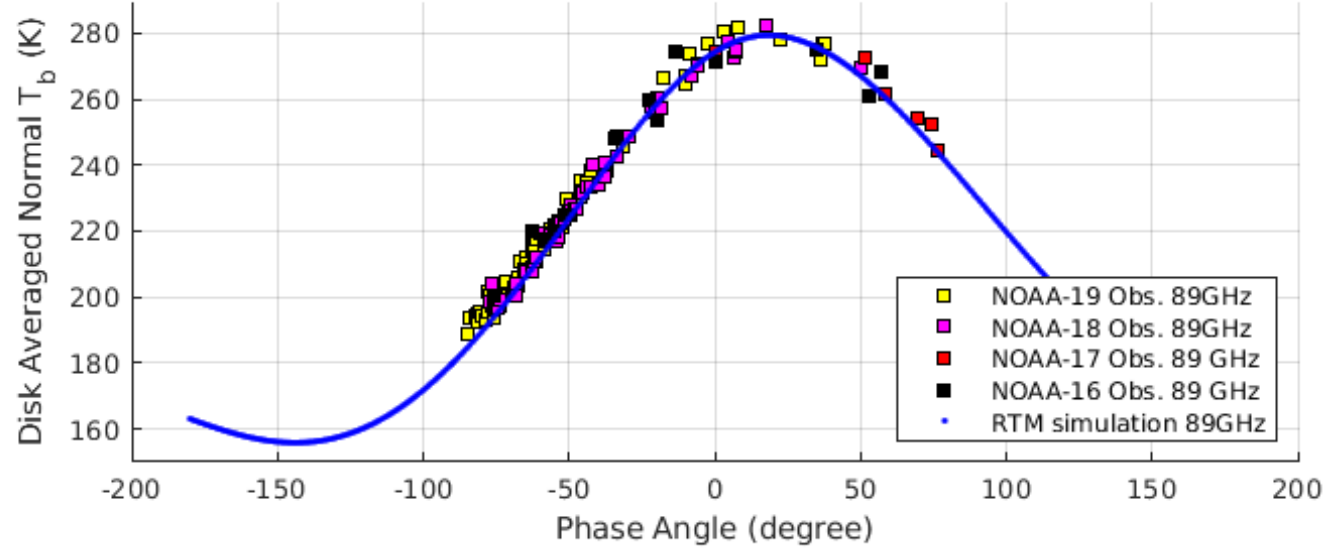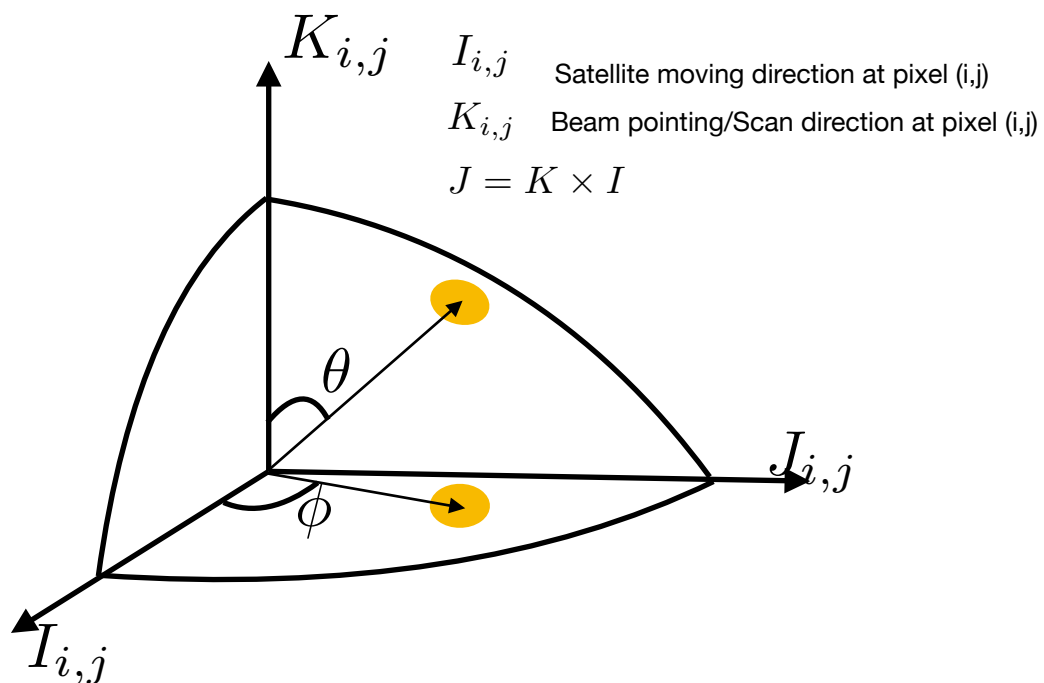Comparison of simulated and observed lunar disk averaged brightness temperature at frequencies of 89~GHz and higher. Solid lines are our model simulations, the dots are the satellite observations with AMSU-B and MHS.

Sat.	Instr.	GHz	Mean Error $Tb^{sat} - Tb^{effsim}$ (K)	Mean Error $Tb^{sat} - Tb^{Fresnel}$ (K)	Std.(K)
N15	AMSU-B	89	-0.7	18.5	9.2
N16	AMSU-B	89	-2.2	16.4	6.7
N17	AMSU-B	89	11	30.3	6.4
N18	MHS	89	4.9	22.5	3.6
N19	MHS	89	6.4	24.1	4.3
M-A	MHS	89	6.4	25.8	5.1
MB	MHS	89	2.8	22.2	3.4
MC	MHS	89	11.3	30.9	7.9
N15	AMSU-B	150	17	36.8	22.2
N16	AMSU-B	150	23.2	42	10
N17	AMSU-B	150	9.6	28.8	22.4
N18	MHS	157	-6.6	11.2	7.2
N19	MHS	157	1.6	19.4	5.2
MA	MHS	157	-2.7	16.8	9.1
MB	MHS	157	-6.1	13.2	4.2
MC	MHS	157	-2	17.6	8.7
N15	AMSU-B	183	10.2	30.2	16
N16	AMSU-B	183	10.4	28.6	10.4
N17	AMSU-B	183	-2.2	16.8	17.3
N18	MHS	183/190	4.4	22.1	4.1
N19	MHS	183/190	2.3	20.1	6.6
MA	MHS	183/190	4.7	24.1	6.1
MB	MHS	183/190	0.7	19.9	3.5
MC	MHS	183/190	13.3	32.8	13.7

Retrieval of Disk-Averaged Moon Tb from Calibrated 2-D Lunar Observations

$I_{i,j}$ Satellite moving direction at pixel (i,j)

$K_{i,j}$ Beam pointing/Scan direction at pixel (i,j)

$J = K \times I$

- The beam pointing error is corrected for the Tb retrieval
- The smearing effect has been taken into account to calculate the lunar solid angle
- Regression algorithm was used for the lunar Tb retrieval
- Observations from adjacent channels with similar frequencies were combined for the retrieval

Regression model for Tb retrieval

$$Ta_{moon}(\theta_{ifov}, \phi_{ifov}) = Tb_{moon}^{Disk} \cdot \frac{\Omega_{moon}^{ifov}}{\Omega_P}$$

$$\Omega_{moon}^{ifov} = \frac{1}{L} \int_{\frac{-\tau}{2}}^{\frac{\tau}{2}} dl \int_{0}^{2\pi} \int_{0}^{\alpha_{moon}} G'(\theta', \phi') \sin\theta' d\theta' d\phi'$$

Channel-Averaged Moon Tb

Band	Frequen	N20	N21
K	23.80	241.21	250.60
Ka	31.40	244.14	255.30
V	50.30	264.44	264.50
W	88.20	274.38	274.90
G1	165.50	289.19	288.50
G2	183.31	293.17	285.40

Disk-Averaged Moon Tb Spectrum from N20 and N21 ATMS
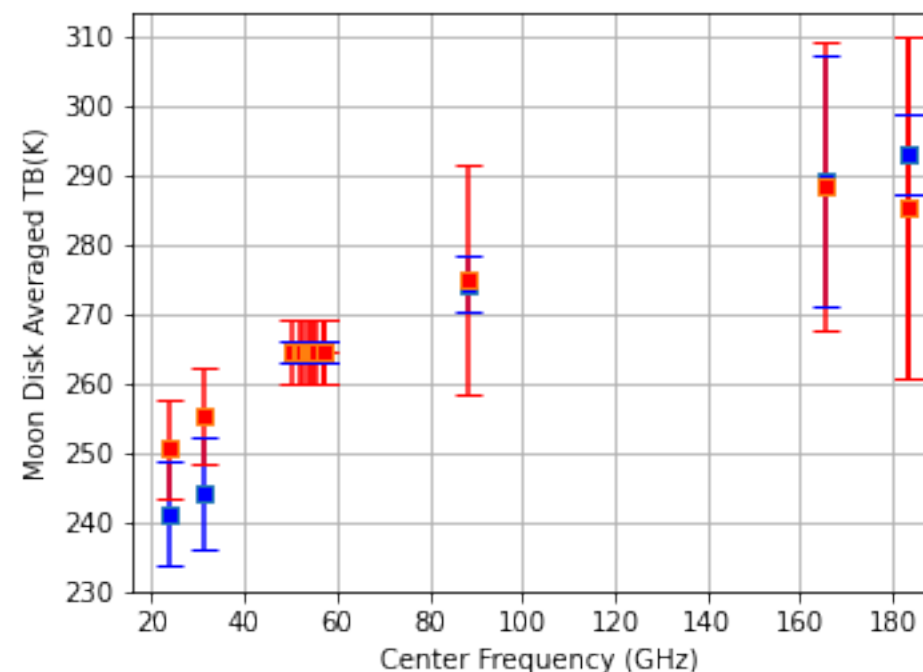
■ NOAA-20 lunar antenna temperature

■ NOAA-21 lunar antenna temperature

Beam Pointing Error Evaluation

NOAA-21 Lunar Geolocation Error Evaluation

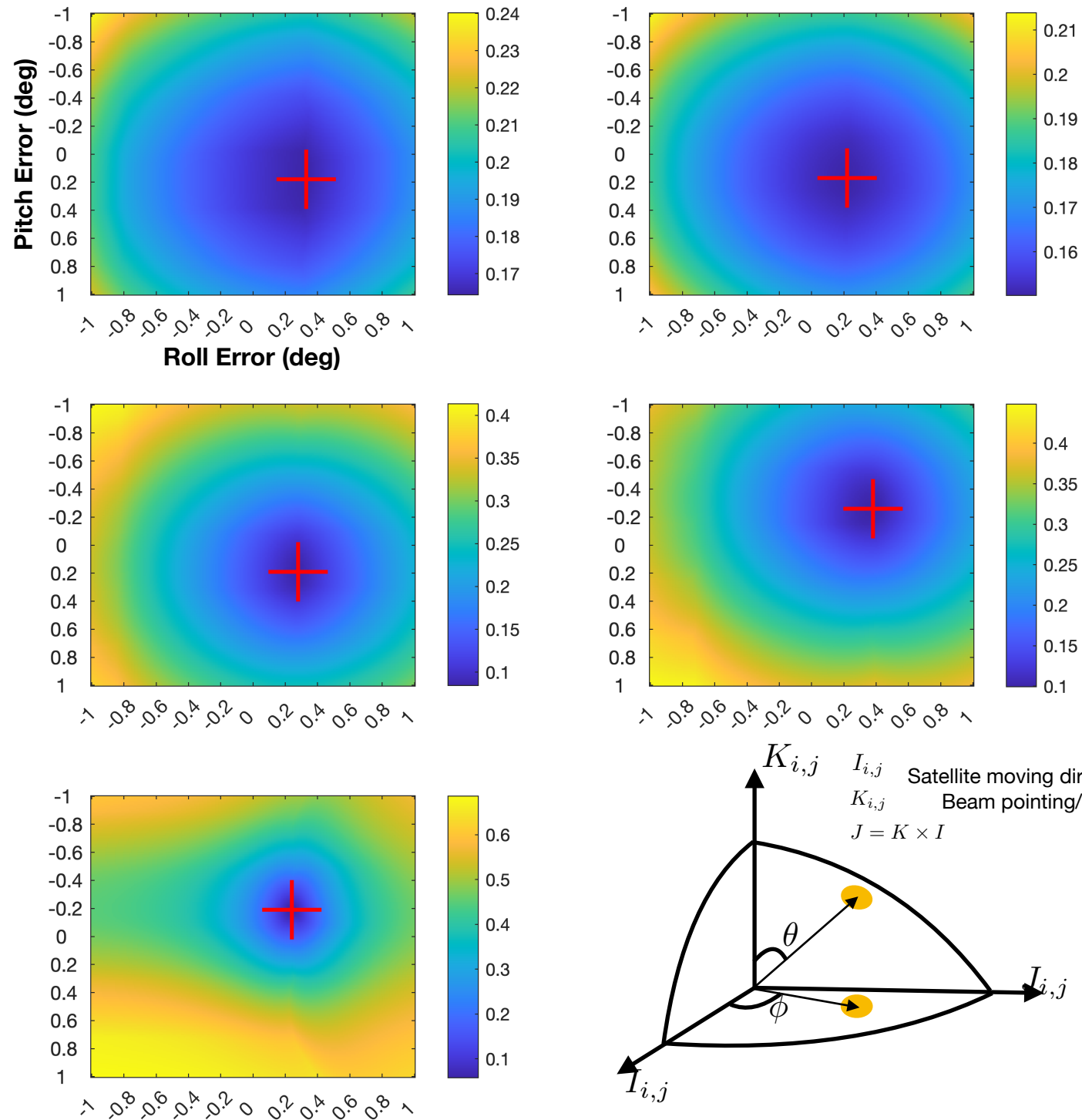Considering the facts that the magnitude of antenna response is very sensitive to position of Moon's center in the Field of View of antenna beam on observing direction. Especially when lunar appears at the center of FOV, where the gradient of antenna response reaches its maximum. Therefore by comparing simulated antenna response of lunar scans with the observation truth, the displacement of beam center can be identified.

$$\sigma(\xi_r, \xi_p) = \frac{1}{N-1} \sqrt{\sum_{i=1}^{N} (G(\xi_r, \xi_p) - G_{obs})^2}$$

To calculate the antenna gain of the moon, the smearing effects need to be taken into account

$$G(\xi_r, \xi_p) = \frac{G_{imoon}}{G_{imoon}^{max}}$$

$$G_{imoon} = \frac{1}{L} \int_{\frac{-\tau}{2}}^{\frac{\tau}{2}} dl \int_{0}^{2\pi} \int_{0}^{\alpha_{moon}} G'(\theta', \phi') sin\theta' d\theta' d\phi'$$

FY-3C MWHS-II

SICS
Global Space-based
Inter-Calibration System

180±2º
Hot Targets

accelerate

270º

90º

MWHS scan sequence

287±2º
Cold Space

earth scene

306.65º

53.35º

0º(Nadir)

FY3C_MWHSX_GBAL_L1_20151002_0101_015KM_MS_SP_CH7

First
Second
Third

10100
10000
9900
9800
9700
9600
9500

01:09   01:24   01:39   01:54   02:09   02:24   02:39

20151002   20151002

$2\theta_{3dB}$
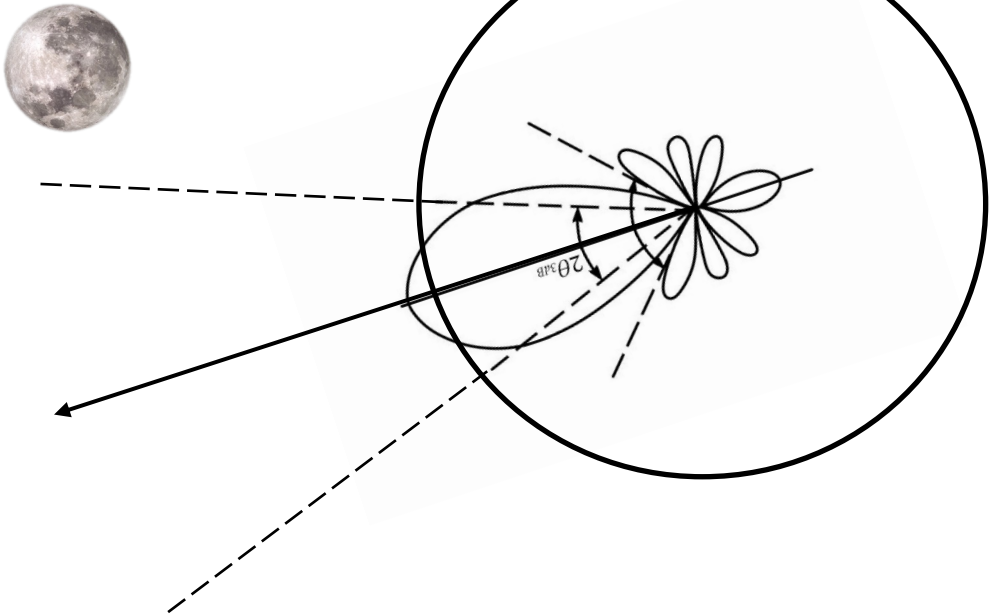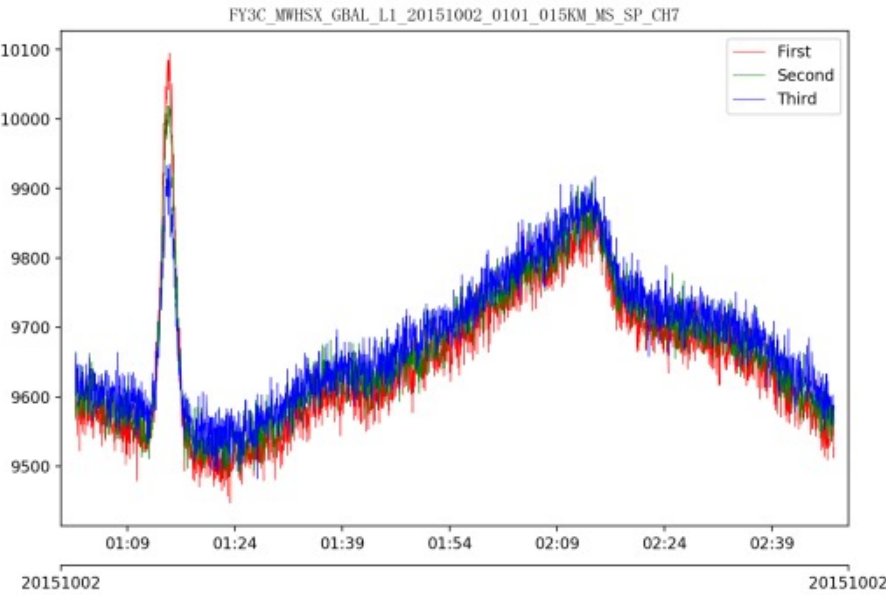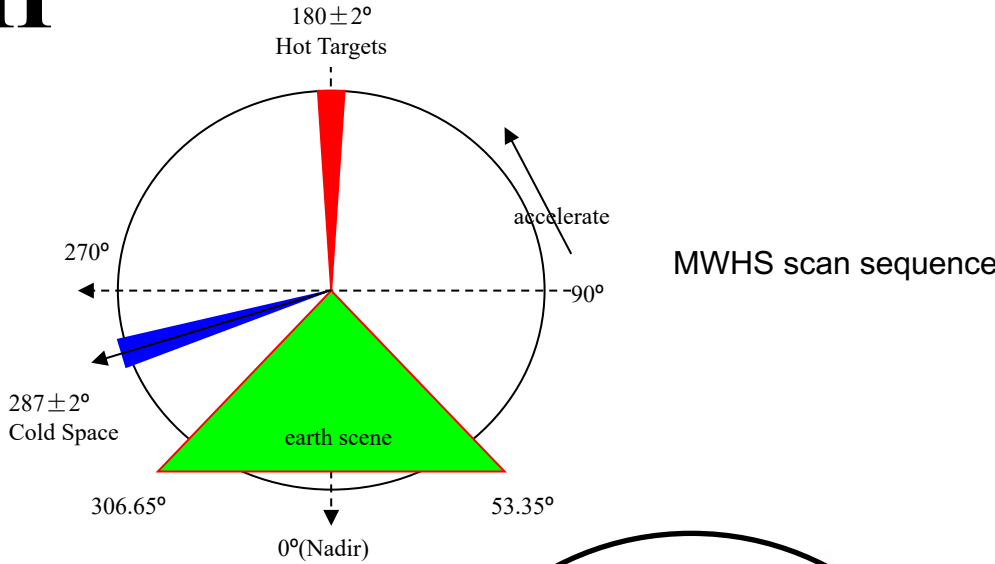
The Moon may occasionally appear in the deep space view (DSV) during certain scans

3

Future Missions with Microwave Radiometers

Mission	Satellites	Instrument	Frequencies	Lunar Intrusion Strategy
EPS–SG	Metop–SG A1 of3	MWS	23.8–229 GHz	Detect + Correct
	Metop–SG B1 of3	MWI ICI	18.7–183 GHz 183–664 GHz	Detect + (Optionally) Correct
Copernicus Sentinel (Joint with ESA)	Sentinel–3C	MWR	23.8+36.5 GHz	No space views! Never see Moon in normal operations
	Sentinel–3D	MWR	23.8+36.5 GHz	
	Sentinel–3 NG	TBD	TBD	
	Sentinel–6B +NG "JASON-CS-B"	AMR–C	18.7–34 GHz	
EPS–Sterna	Sterna	MWR (AWS)	50–325 GHz	Flag by geometry + stats
Copernicus Expansion (Joint with ESA)	CIMR–1/2 (06/18)	CIMR	1.4–36.5 GHz	ESA responsible for L1 Manoeuvres to view space Correct for Moon – TBC

EPS-SG/MWS

- Flag for Moon contamination correction of each Space View position
  - Threshold for difference between lunar angle and antenna space view
  - for which the data are flagged as calibration contaminated
- MWS has 5 space views
  - Not all usually contaminated – just used unflagged ones
- Optionally apply possible correction (in case all views contaminated):
  - Apply to cleanest Space View – with lowest count
  - Follow Yang et al. 2018, BT of Moon:

$$T'_{B,moon}(j) = v_{tb_{moon},0}(j) +$$
$$+v_{tb_{moon},1}(j) \cdot [1 - cos(\theta_{sun_{moon}})] + v_{tb_{moon},2}(j) \cdot [1 + cos(2 \cdot \theta_{sun\_moon})]$$

  - in channel, j, as function of function of the angle between Sun and Moon
  - With coefficients $v_{tb_{moon},}$
  - Convert BT into radiances using the Planck function
  - Convolve with Antenna Pattern to define antenna efficiency
  - Calculate solid angle for Moon disc
  - Simplify by assuming Gaussian to calculate **δR_moon** – see below
  - Subtract lunar radiance from corresponding space view radiance
  - Use corrected space view radiance in calibration as usual
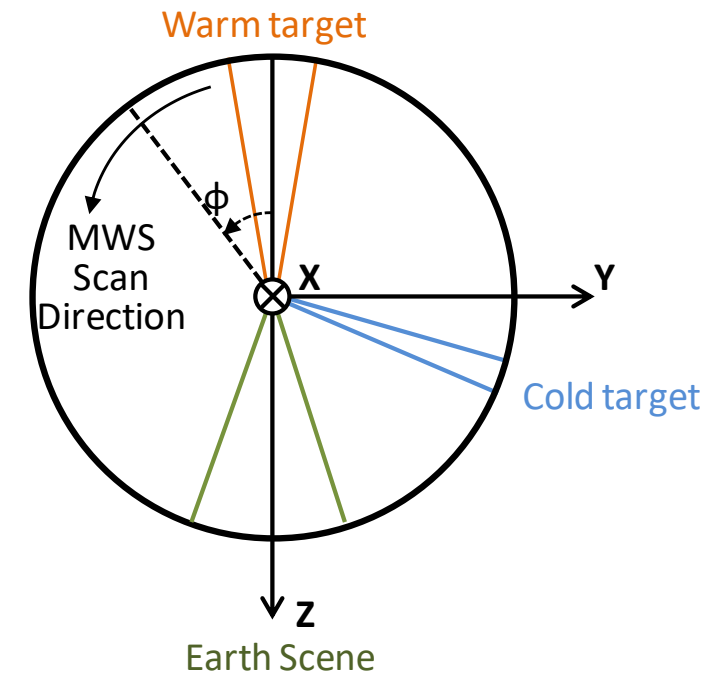
Figure 1. MWS calibration strategy (adapted from [MWS-IRS]).

$$\delta R^{\square}_{c,moon}(j) = \left(\pi \cdot \delta\zeta_{moon}^2\right) \cdot \frac{e^{-\frac{\left(\zeta_{coldview\_moon}(i_{FOV\_cal})\right)^2}{2 \cdot \left(\frac{\Theta^{cold}_{HPBW}(i_{sp\_p},i_{FOV_{cold_{moon}}},j)}{2\sqrt{2\,ln(2)}}\right)^2}}}{2\pi \cdot \left(\frac{\Theta^{cold}_{HPBW}(i_{sp\_p},i_{FOV_{cold_{moon}}},j)}{2\sqrt{2\,ln(2)}}\right)^2} \cdot R^{bb}_{moon}(j)$$

EPS-SG/MWI+ICI

- MWI and ICI are conical-scanning systems
- View cold sky every scan through Space View Reflector
- Per scan cycle MWI has 38 space samples over ~4° validity window, 28 for ICI over ~5°
  - Not all usually contaminated by Moon intrusion

Detection:

- Flag for Moon contamination correction of each Space View position
  - Threshold (currently set to 2°) for angle difference in SVR frame between:
    – unit vector centred on the Moon and directed to the satellite (Moon angle)
    – unit vector pointing in the boresight direction of the SVR
 - Flagged space samples are not used for calibration, use only the unflagged ones.

Correction (descoped for Day 1, applicability to conically scanners to be demonstrated):

- Follows Mo and Kigawa (2007) method:
1) The band-average BT of Moon for scan i as function of the angle between Sun and Moon is
$$TB_{moon}(i) = 95.21 + 104.63 \cdot [1 - cos(\theta_{sun\_moon}(i))] + 11.62 \cdot [1 + cos(2 \cdot \theta_{sun\_moon}(i))]$$
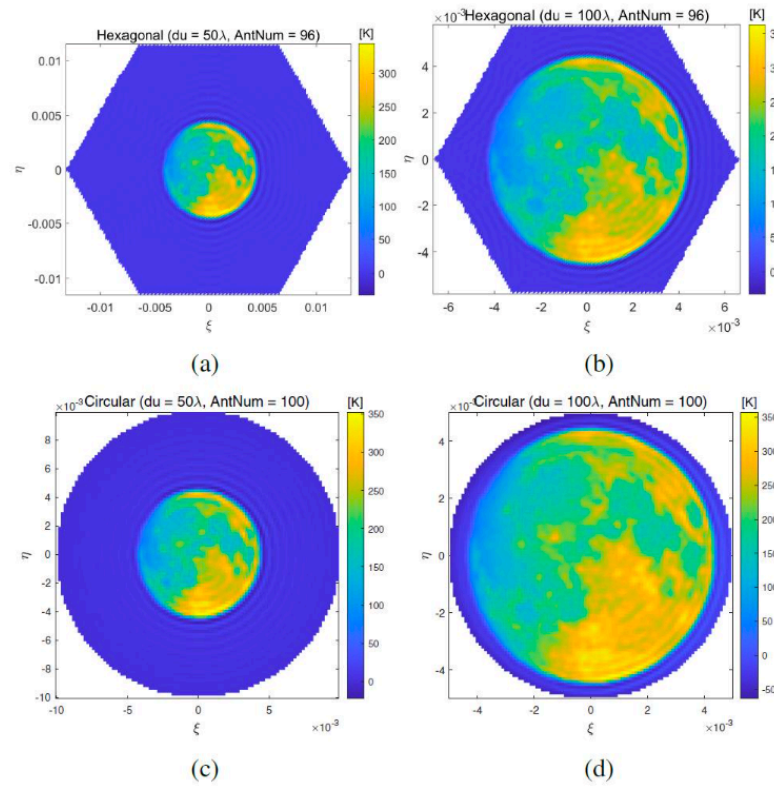2) Apply Band-average correction:
$$TB'_{moon}(i,j) = c(j) \cdot TB_{moon}(i) + b(i)$$
3) Convert BT into radiance R_{moon} using the Planck function.
4) Compute Moon Radiance contribution to cold space radiance: $\Delta R_C(i, k, j) = G \cdot \beta(j) \cdot d_{r(i)} \cdot R_{moon}(i,j)$
   with: G is antenna pattern function corresponding to Moon position in the SVR frame
   β is area ratio of the Lunar disk, computed pre-launch

   d_r is moon correction distance ratio , $d_r(i) = \left(\frac{d_0}{d(i)}\right)^2$

   d_0 is average Moon-Earth distance, d Is the Moon-satellite actual distance
5) The moon count correction ΔC_C is calculated from $\Delta R_C(i, k_c, j)$: $\Delta C_C(i, k, j) = \left[\dfrac{\bar{C}_H(i,j) - C_C(i, k, j)}{R_H^{eff}(i,j) - \left(R_C^{eff}(i,k,j) + \Delta R_C(i,k,j)\right)} \right] \Delta R_C(i,k,j)$
6) The contaminated cold counts are then corrected:
$$C_C(i,k,j) = C_C(i,k,j) - \Delta C_C(i,k,j)$$

MWI basic repeat cycle
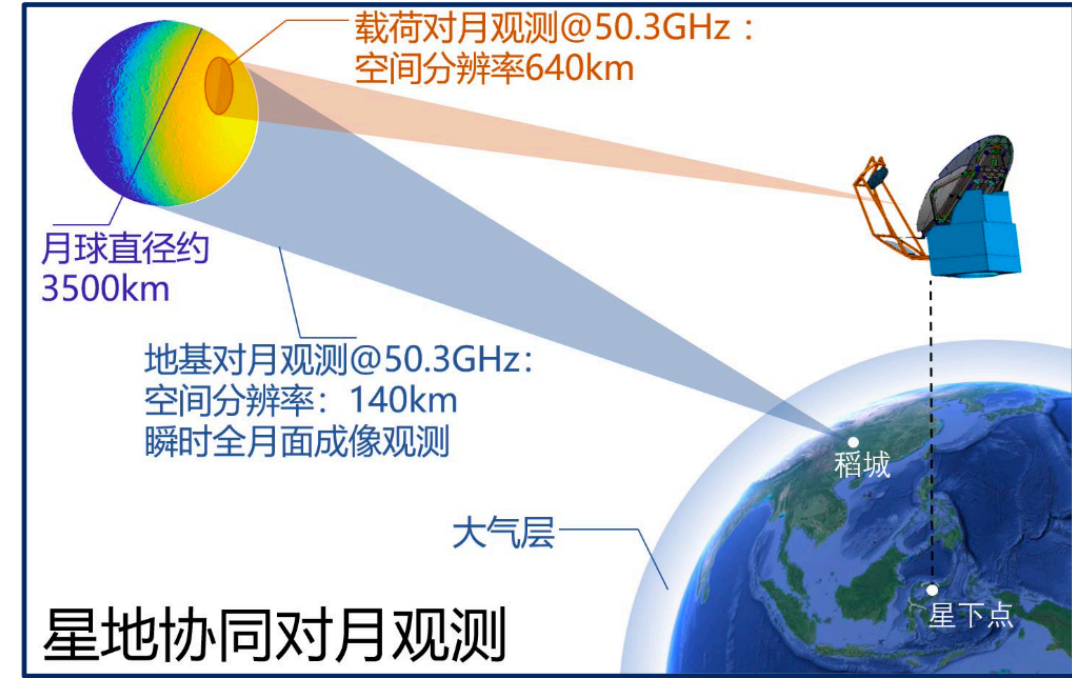

ICI basic repeat cycle
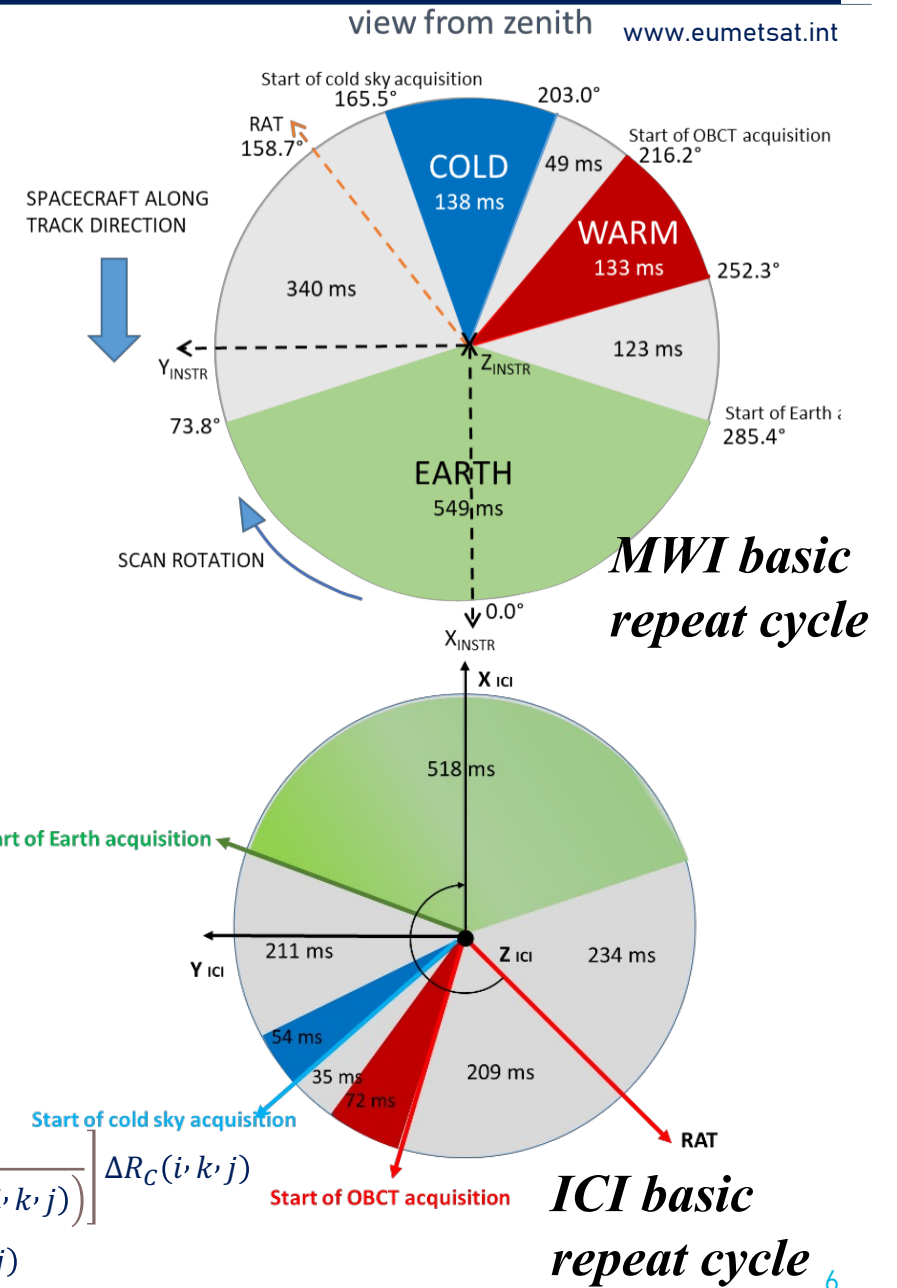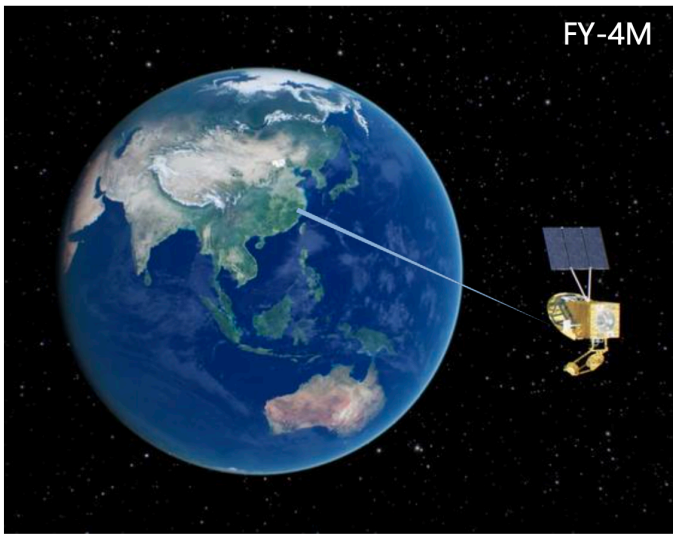
FY-4M

K. Chen, Z. Suo, W. Han and B. Cai, "OSSEs on the FY-4M Geostationary Microwave Satellite Based on CMA-GFS and CMA-MESO," in IEEE Transactions on Geoscience and Remote Sensing, vol. 62, pp. 1-19, 2024
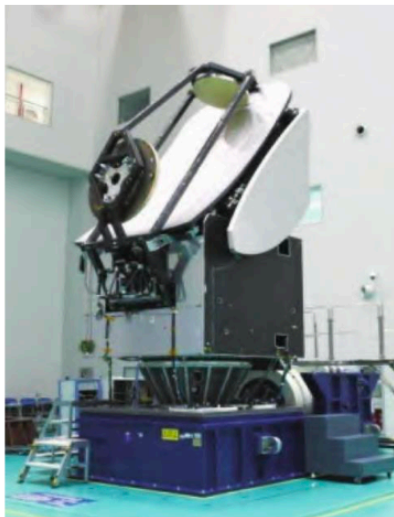

(a) Hexagonal (du = 50λ, AntNum = 96)　(b) Hexagonal (du = 100λ, AntNum = 96)
(c) Circular (du = 50λ, AntNum = 100)　(d) Circular (du = 100λ, AntNum = 100)

Simulated ground-based observation

(Provided by Dr. Hao Liu)

载荷对月观测@50.3GHz：空间分辨率640km

月球直径约3500km

地基对月观测@50.3GHz：空间分辨率：140km 瞬时全月面成像观测
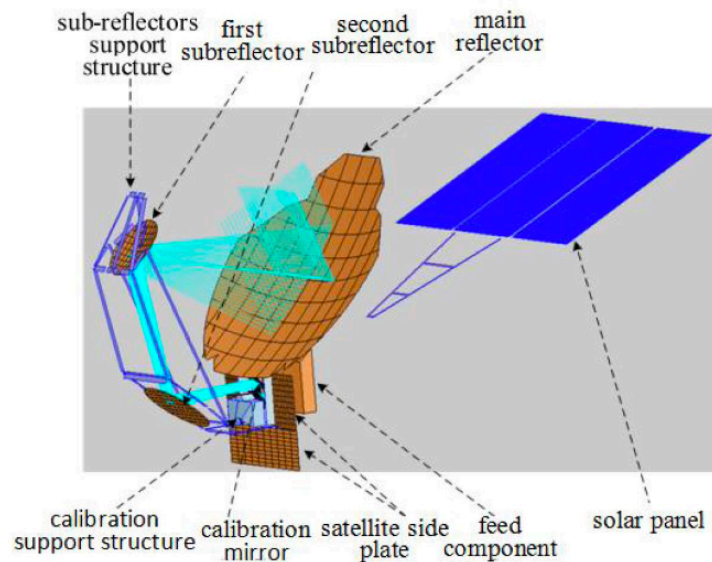
大气层

稻城

星下点

星地协同对月观测

FY-4M MM wave & sub-MM wave Radiometer

☐ ~5 meter reflector, 23.8~424GHz

☐ Periodical calibration with a scanning mirror after the second sub-reflector


Principle model of FY-4M

sub-reflectors support structure　first subreflector　second subreflector　main reflector

calibration support structure　calibration mirror　satellite side plate　feed component　solar panel

| No.	Center frequency (GHz)	Bandwidth (MHz)	Pol	Sensitivity (K)	Measurement Accuracy (K)	Spatial resolution (km)
1	23.8	270	V	0.5	1.5	≤130
2	23.8	270	H	0.5	1.5	≤130
3	31.4	180	V	0.5	1.5	≤110
4	31.4	180	H	0.5	1.5	≤110
5	50.3	180	V	0.5	1.5	≤60
6	50.3	180	H	0.5	1.5	≤60
7	51.76	400	H	0.5	1.5	≤60
8	52.8	400	H	0.5	1.5	≤60
9	53.246±0.080	2*140	H	0.5	1.5	≤60
10	53.596±0.115	2*170	H	0.5	1.5	≤60
11	53.948±0.081	2*142	H	0.5	1.5	≤60
12	54.4	400	H	0.5	1.5	≤60
13	54.94	400	H	0.5	1.5	≤60
14	55.5	330	H	0.5	1.5	≤60
15	57.290344(f0)	330	H	1	2	≤60
16	f0±0.217	2*78	H	1	2	≤60
17	f0±0.322±0.048	4*36	H	1	2	≤60
18	f0±0.322±0.022	4*16	H	1.5	2	≤60
19	f0±0.322±0.010	4*8	H	1.5	2	≤60
20	f0±0.322±0.0045	4*3	H	2.5	2.5	≤60
21	89	3000	V	0.5	1.5	≤40
22	118.75±0.08	2*20	H	2.5	2.5	≤40
23	118.75±0.2	2*100	H	1.5	1.5	≤40
24	118.75±0.3	2*165	H	1	1.5	≤40
25	118.75±0.8	2*200	H	1	1.5	≤40
26	118.75±1.1	2*200	H	1	1.5	≤40
27	118.75±2.5	2*200	H	1	1.5	≤40
28	118.75±3.0	2*1000	H	1	1.5	≤40
29	118.75±5.0	2*2000	H	1	1.5	≤40
30	165.5	2800	V	1	1.5	≤25
31	183.31±11	2*2000	H	0.5	1.5	≤25
32	183.31±7.0	2*2000	H	0.5	1.5	≤25
33	183.31±4.5	2*2000	H	0.5	1.5	≤25
34	183.31±3.0	2*1000	H	1	1.5	≤25
35	183.31±1.8	2*1000	H	1	1.5	≤25
36	183.31±1.0	2*500	H	1	1.5	≤25
37	229	2000	V	1	1.5	≤25
38	380.197±18.0	2*2000	H	1	2	≤25
39	380.197±9.0	2*2000	H	1	2	≤25
40	380.197±1.5	2*500	H	2	2	≤25
41	380.197±0.4	2*200	H	2.5	2	≤25
42	424.763±4.0	2*1000	H	1	2	≤17
43	424.763±1.5	2*600	H	1.5	2	≤17
44	424.763±1.0	2*400	H	2	2	≤17
45	424.763±0.6	2*200	H	2.5	2	≤17
46	424.763±0.3	2*100	H	3	2	≤17

Ground-based Microwave Lunar Observation: Circular Interferometric Array NSSE

(Provided by Dr. Hao Liu)

☐ Frequency band: window channel, 31.4/50.3/89GHz

☐ Instrument Type: Synthetic Aperture Interferometric Radiometer

- Circular Array to achieve low side-lobe and suppress the aliasing contribution of atmosphere
- Periodical end-to-end amplitude calibration with external calibration targets
- Inter-element phase calibration achieved by redundant baseline measurements

☐ Site selection: Daocheng, Sichuan Province
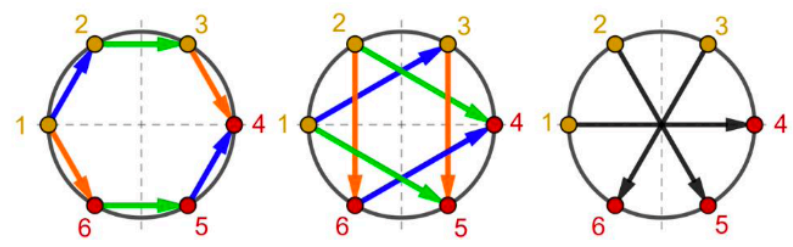
X. Guo, A. Camps, H. Park, H. Liu, C. Zhang and J. Wu, "Phase and Amplitude Calibrations of Rotating Equispaced Circular Array for Geostationary Microwave Interferometric Radiometers — Theory and Methods," IEEE TGRS, vol. 60, 2022
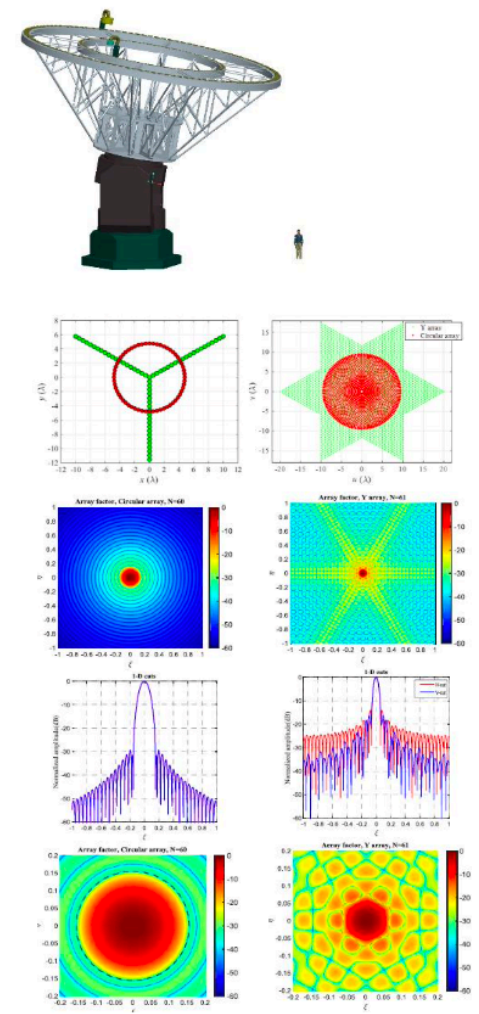
J. Wu, C. Zhang, H. Liu and J. Yan, "Performance Analysis of Circular Antenna Array for Microwave Interferometric Radiometers," IEEE TGRS, vol. 55, 2017

Specifications	Ground-based Observation			FY-4M		
Frequency Band (GHz)	31.4	50.3	89	31.4	50~57	89
Array/Reflector Size (m)	≥15	≥15	≥7	5	5	~3
Frequency stability (MHz)	≤0.1	≤0.1	≤10	± 0.5	± 0.5	± 50
Angular resolution (°)	≤0.04°	≤0.02°	≤0.02°	0.19°	0.09°	0.06°
Spatial resolution on lunar surface(km)	≤280	≤140	≤140	1280	640	420
FOV (°)	≥0.53°	≥0.53°	≥0.53°	/	/	/
NEDT(K)	0.35K@2min	0.35K@2min	0.35K@2min	0.5	0.5	0.5
Calibration Accuracy(K)	≤1	≤1	≤1	1.5	1.5	1.5